Increase in beta frequency phase synchronization and power after a session of high frequency repetitive transcranial magnetic stimulation to the primary motor cortex

De Martino, Enrico; Casali, Adenauer Girardi; Nascimento Couto, Bruno Andry; Graven-Nielsen, Thomas; Ciampi de Andrade, Daniel

Published in:
Neurotherapeutics

DOI (link to publication from Publisher):
10.1016/j.neurot.2024.e00497

Publication date:
2025

Document Version
Publisher's PDF, also known as Version of record

Neurotherapeutics 22 (2025) e00497

Contents lists available at ScienceDirect

Neurotherapeutics

journal homepage: www.sciencedirect.com/journal/neurotherapeutics

Original Article

Increase in beta frequency phase synchronization and power after a session of high frequency repetitive transcranial magnetic stimulation to the primary motor cortex

Enrico De Martino [a], Adenauer Girardi Casali [b], Bruno Andry Nascimento Couto [a], Thomas Graven-Nielsen [a], Daniel Ciampi de Andrade [a,*]

[a] Center for Neuroplasticity and Pain (CNAP), Department of Health Science and Technology, Faculty of Medicine, Aalborg University, Aalborg, Denmark
[b] Institute of Science and Technology, Federal University of São Paulo, São Paulo, Brazil

ARTICLE INFO

Keywords:
Transcranial magnetic stimulation
Electroencephalogram
Time-frequency analysis
Phase reset
Primary motor cortex

ABSTRACT

High-frequency repetitive transcranial magnetic stimulation (rTMS) to the primary motor cortex (M1) is used to treat several neuropsychiatric disorders, but the detailed temporal dynamics of its effects on cortical connectivity remain unclear. Here, we stimulated four cortical targets used for rTMS (M1; dorsolateral-prefrontal cortex, DLPFC; anterior cingulate cortex, ACC; posterosuperior insula, PSI) with TMS coupled with high-density electroencephalography (TMS-EEG) to measure cortical excitability and oscillatory dynamics before and after active- and sham-M1-rTMS. Before and immediately after active or sham M1-rTMS (15 min, 3000 pulses at 10 Hz), single-pulse TMS-evoked EEG was recorded at the four targets in 20 healthy individuals. Cortical excitability and oscillatory measures were extracted at the main frequency bands (α [8–13 Hz], low-β [14–24 Hz], high-β [25–35 Hz]). Active-M1-rTMS increased high-β synchronization in electrodes near the stimulation area and remotely, in the contralateral hemisphere ($p = 0.026$). Increased high-β synchronization (48–83 ms after TMS-EEG stimulation) was succeeded by enhancement in low-β power (86–144 ms after TMS-EEG stimulation) both locally and in the contralateral hemisphere ($p = 0.006$). No significant differences were observed in stimulating the DLPFC, ACC, or PSI by TMS-EEG. M1-rTMS engaged a sequence of enhanced phase synchronization, followed by an increase in power occurring within M1, which spread to remote areas and persisted after the end of the stimulation session. These results are relevant to understanding the M1 neuroplastic effects of rTMS in health and may help in the development of informed rTMS therapies in disease.

Introduction

High-frequency (10 Hz) repetitive transcranial magnetic stimulation (rTMS) to the primary motor cortex (M1) is a non-invasive neuromodulation technique known to produce therapeutic benefits in various conditions, including movement disorders, stroke rehabilitation, and chronic pain [1]. RTMS is believed to induce long-lasting cortical plastic changes by repetitively depolarizing myelinated axons within M1 [2], probably via Hebbian synaptic plasticity mechanisms [3]. While studies based on motor-evoked potentials (MEPs) and intra-cortical excitability showed that 10 Hz M1 rTMS increased corticospinal motor excitability [4], others found variable effects depending on protocol types and inter-individual differences [5,6].

Recent advancements in TMS-compatible electroencephalography (TMS-EEG) have opened the possibility of directly assessing cortical responses to pulses of TMS both at the stimulation site (i.e., excitability) and remotely, which can open new perspectives in studying the dynamics of the effects of M1 rTMS on cortical oscillatory activity in detail. TMS-EEG involves the application of sub-threshold TMS single pulses to a targeted cortical area under the recording of EEG to assess the ensuing changes in cortical neural activity [7], and allows for the measurement of cortical excitability and connectivity with enough temporal resolution to early and later evoked responses in motor and extra-motor areas [8]. Averaged cortical responses, known as TMS-evoked EEG potentials (TEPs), are waveforms derived from EEG segments time- and phase-locked to TMS pulses, which are particularly effective for

* Corresponding author.
E-mail address: dca@hst.aau.dk (D. Ciampi de Andrade).

https://doi.org/10.1016/j.neurot.2024.e00497
Received 21 July 2024; Received in revised form 6 October 2024; Accepted 14 November 2024

examining cortical excitability [9]. Furthermore, TMS-EEG also allows for the exploration of the frequency content of evoked cortical oscillations both locally in the stimulated area and globally across cortical regions connected to the stimulated cortical target [8].

The dominant oscillatory EEG spectrum over M1 is the β-band [10,11], which involves pyramidal neurons, as evidenced by corticomuscular coherence studies [12]. However, M1 also expresses an important oscillatory activity within the α-band, also termed mu-rhythm, which is related to the integration of somatosensory stimuli in a manner like the modulation of visual perception by occipital α oscillations [13]. Previous studies combining TMS-EEG to continuous theta burst stimulation (TBS) of M1 have shown a significant increase in power in beta frequency [14] and a reduction in alpha power and phase synchronization in the stimulation site [14,15]. By contrast, intermittent TBS has reported a decrease in power in α-band frequencies in the electrodes located away from the stimulation site [16]. Studies assessing the changes of M1 rTMS to M1 on functional magnetic resonance imaging (fMRI) have also demonstrated changes in BOLD signal in functionally connected cortical non-motor regions, such as the insular, prefrontal, and cingulate regions [17,18]. However, how high-frequency M1 rTMS affects power and phase-based activity locally and remotely within the cortex remains largely unknown. It also remains unknown whether the potential cortical changes occurring after rTMS to M1 can persist after the end of stimulation, and if they do, what their profiles are.

M1 is highly connected to cognitive, affective, and somatosensory networks [19]. It is currently known that M1 stimulation has significant neuromodulatory effects in extra-motor corticospinal networks [20]. However, to date, the dynamics of rTMS to M1 have not been comprehensively explored over extra-motor areas using techniques with optimal temporal resolution. For example, the posterosuperior insula (PSI) is functionally connected to primary and secondary motor and somatosensory cortices [21], and functional correlations between these regions, likely mediated through thalamic relays or other intermediary regions, have been described [22]. Moreover, 10Hz-rTMS to the PSI has been shown to change remote motor cortical excitability under TMS-EEG in parallel with its expected analgesic effects [23]. Similarly, the anterior cingulate cortex (ACC) is also strongly interconnected with M1 and is known to integrate motivational aspects of behavior and influence motor comportment [24]. The dorsolateral prefrontal cortex (DLPFC) plays a crucial role in cognitive control of motor behavior [25]. Although there are no direct anatomical connections between DLPFC and M1, TMS studies have demonstrated coupling between the two regions in the millisecond timescale [26,27]. Understanding the roles of these functionally connected areas in M1 modulation could provide deeper insights into the network effects of rTMS on both motor and extra-motor regions.

Here, we investigated whether M1-rTMS influenced cortical excitability and oscillatory dynamics within the α- and β-bands in humans by stimulating local motor (M1) and extra-motor (DLPFC, ACC, and PSI) cortices with TMS-EEG before and after M1 rTMS in a sham-controlled setting. It is hypothesized that 10 Hz rTMS to M1 would lead to an increase in cortical excitability and enhanced oscillatory dynamics within the α- and β-bands, both locally in the motor cortex and interconnected extra-motor regions, reflecting modulation across functional brain networks.

Methods

Participants

This study included 20 healthy adults (12 females). Age, height, and weight (mean ± SD) were 25 ± 4 years, 173 ± 12.6 cm, and 67 ± 15 kg. None of the participants were on medications, and the exclusion criteria were non-systemic diseases and neuropsychiatric disorders, known pregnancy, and any contraindications to TMS [28]. The local ethics committee approved the study (N-20220018), and the protocol was registered at ClinicalTrials.gov (NCT05714020).

Study design

The present study involved two experimental sessions separated by at least one week. In the first visit, participants were randomly assigned to either sham or active rTMS to the left M1, with 10 participants receiving sham rTMS first. All participants received the other rTMS protocol during the second visit. Both active and sham rTMS procedures, as well as participant instructions, were kept consistent across groups. Before and within 1 h after the active or sham rTMS intervention, TMS-EEG assessments were performed on four distinct cortical areas of the left hemisphere: first, the M1 and DLPFC regions were stimulated in a randomized order in all 20 participants (10 receiving DLPFC stimulation first), then either ACC or PSI was stimulated (in 10 participants for each region). Each TMS-EEG protocol took approximately 8 min for each cortical target, and 5-min breaks were ensured between runs.

To collect the post-measurement assessments within 1 h after rTMS, half of the participants underwent TMS-EEG to the anterior cingulate cortex (ACC), while the second half underwent the posterosuperior insula (PSI). MEPs were measured both before TMS-EEG (approximately 1 h and 30 min before rTMS) and 1 h after rTMS (Fig. 1). This experimental design was made to ensure that the entire post-rTMS assessment period remained within a 1-h window, as changes in MEPs after rTMS are typically short-lasting [29]. Measuring both the ACC and PSI in all participants would have extended the post-measurement period beyond this time frame, potentially obscuring any transient effects of rTMS on cortical excitability.

Repetitive transcranial magnetic stimulation

Magstim Super Rapid$_2$ Plus$_1$ stimulator (Magstim Company Ltd) with a figure-of-eight-shaped coil (70-mm Double Air Film Coil) was used for rTMS (15 min of stimulation, targeting the hot spot of the right first dorsal interosseous (FDI) muscle, 30 trains of 10-s pulses at 10 Hz frequency and 20-s intervals between trains, totaling 3000 pulses) [1]. Stimulation intensity was 90 % of the resting motor threshold (rMT). For sham stimulations, a coil identical in size, color, shape, and mimicking the active coil sound (70-mm double air film sham coil) was used.

Resting motor threshold and MEP size measurement

The rMT was measured at the motor hotspot both on the right FDI and TA muscles using D70^2 and D110, respectively, but only MEP size recruitment was assessed for the right FDI muscle at 120 % and 140 % of FDI-rMT using D70^2. Silver chloride electrodes (Ambu Neuroline 720) were placed on the right FDI muscle fibers. The hotspot of the FDI muscle was determined as the coil position that evoked a maximal peak-to-peak MEP for a given stimulation intensity. The rMT was the lowest TMS intensity that could produce MEPs exceeding 50 μV in half of the trials [30]. Ten pulses were delivered at 120 % and 140 % of rMT.

Electroencephalographic recordings of TMS-evoked potentials

Electroencephalograms were recorded using a TMS-compatible amplifier (g.HIamp EEG amplifier, g.tec medical engineering GmbH) with a passive electrode cap (64 electrodes, Easycap) placed according to the 10-5 system, with the Cz electrode on the vertex. The ground electrode was placed on the right zygoma, the online reference was on the right mastoid process, and two electrodes on the lateral side of the eyes recorded the electrooculogram. Electrode impedance was kept under 5 kΩ. Raw signals were amplified and sampled at a rate of 4800 Hz.

TMS was delivered using the same biphasic stimulator as used for rTMS with a figure-eight coil to stimulate DLPFC and M1 (D70^2 coil) and a double-cone coil (D110 cone-coil) to stimulate the ACC and PSI targets. During recordings, participants sat on an ergonomic armchair and were instructed to gaze at a fixation spot on the wall to reduce oculomotor muscle activity. The TMS-click sound masking toolbox (TAAC; [31]) with noise-cancelation in-ear headphones (ER3C Etymotic 50 Ohm) were used to mitigate auditory

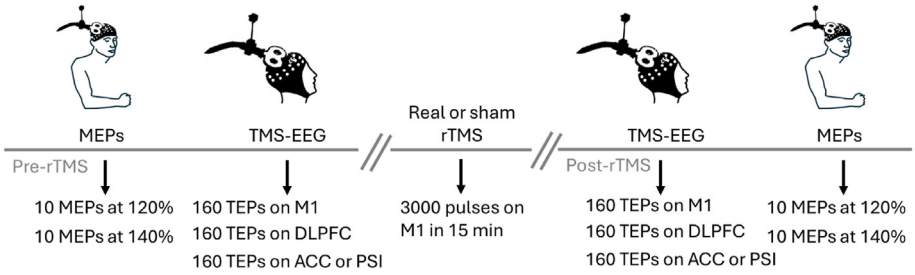

Fig. 1. Before sham or active repetitive transcranial magnetic stimulation (rTMS) to the left primary motor cortex (M1), motor-evoked potentials (MEPs) were recorded at 120 % and 140 % of the resting motor threshold (rMT). TMS-EEG assessments were then performed on the M1 and dorsolateral prefrontal cortex (DLPFC) in randomized order, followed by stimulation of either the anterior cingulate cortex (ACC) or posterosuperior insula (PSI) (with 10 participants assigned to each region). After the 15-min rTMS intervention to M1, TMS-EEG recordings were repeated, followed by the collection of MEPs.

responses to TMS coil clicks. An EEG net cap (GVB-geliMED GmbH) with a plastic stretch wrap film was applied over the EEG cap to reduce somatosensory artifacts triggered by coil contact with electrodes.

TMS-neuronavigation (Brainsight TMS Neuronavigation, Rogue Research Inc.) was used to target the cortical spots between assessments. For M1, TMS-evoked potentials were obtained from motor hotspots (Fig. 2A) at 90 % of rMT. The DLPFC target was identified on the middle

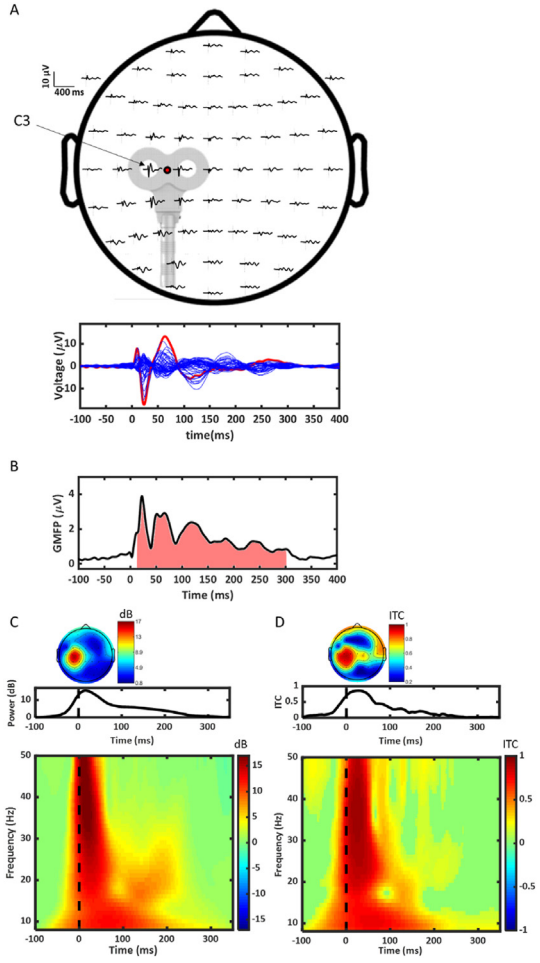

Fig. 2. Sample data of transcranial magnetic stimulation (TMS)-evoked potentials recorded with EEG following single pulse stimulation to the left primary motor cortex (M1) in a representative participant. **A)** Topographical representation of M1 TEPs for each individual electrode. The red dot corresponds to the area of stimulation. The butterfly plot shown below depicts the superposition of TEPs for all electrodes. The red line corresponds to the C3 electrode, and the blue lines correspond to the other 62 channels. **B)** Mean broadband event-related spectral perturbation (ERSP) over time on C3 (time: from −100 to 350 ms). Below is the ERSP map calculated on the same electrode. **C)** Mean broadband inter-trial coherence (ITC) over time on C3 (time: from −100 to 350 ms). Below is the ITC map calculated on the same electrode.

frontal gyrus, based on the method described by Mylius et al. [32], with TMS intensity set to 110 % of the rMT of the FDI muscle (Supplementary Fig. 1A). The ACC target was identified 4 cm in front of the hotspot of the tibialis anterior (TA) muscle scalp representation [33] (Supplementary Fig. 2A). The hotspot of the TA muscle was determined as the coil position that evoked a TA-evoked response for a given stimulation intensity. The rMT of the TA muscle was determined as the lowest TMS intensity to produce visible muscle responses, and TMS-EEG was performed at 90 % of the TA rMT. The PSI target was identified using a previously established and validated fast-PSI formula developed based on neuroanatomical landmarks and functional imaging studies [34]. This method involves first identifying the vertex, which is the intersection of the nasion-inion and tragus-tragus distances on the scalp. Next, the Nasion-PSI line is calculated by multiplying the nasion-inion distance by a correction factor. Similarly, the Vertex-PSI line is calculated by multiplying the vertex-tragus distance by another correction factor. The Fast-PSI target is then located at the intersection of these two lines [34]. The stimulation for PSI was set at 90 % of the TA rMT (Supplementary Fig. 3A).

A real-time visualization tool (rt-TEP) was used to ensure detectable TMS-evoked potentials in all cortical targets [7]. This allowed for monitoring the quality of the recordings and allowed for minor adjustments in TMS coil angulation and orientation, ensuring the presence of early peak-to-peak TMS-evoked potentials (average of 20 trials) at the nearest electrode to the stimulation area. Although the rt-TEP method was originally developed for the figure-of-eight coil, its real-time display of TEPs was extremely useful during data collection in this study. It enabled the optimization of the coil positioning and minimized TMS-associated artifacts. When targeting the PSI, the coil was slightly rotated to avoid direct stimulation of the temporalis muscle, which introduced large muscle artifacts. In the case of the ACC, since the coil was positioned along the midline, it naturally produced fewer muscle artifacts due to the absence of nearby large muscles. Consequently, ACC targeting required minimal adjustments, as it is more distant from muscle interference than other regions.

The TMS-neuronavigation and rt-TEP were utilized throughout the study to monitor the TMS coil location and the highest signal-to-noise ratio in EEG recordings. Approximately 160–180 pulses were administered for each condition, with interstimulus intervals randomly jittered between 2600 and 3400 ms [35].

Pre-processing was performed using customized algorithms based on the EEGlab toolbox [36] running on Matlab R2019b (The MathWorks). EEG signals were segmented into trials of 1600 ms around the TMS pulse, which occurred at time zero (±800 ms). In the M1 TMS-EEG epoch, a segment of the pre-TMS EEG signal (−11 to −3 ms) was used to substitute the peri-TMS EEG recordings from −2 to 6 ms [37]. This time window was chosen as it was sufficiently long to effectively remove the TMS pulse artifacts and part of the decay artifact when present. The same procedure was applied for deep TMS targets (ACC and PSI) in a larger peri-TMS interval (0–20 ms) to adapt to the double-cone coil electric field and any residual artifacts were removed using the independent component analysis (ICA). The Epochs and channels with noise, eye blinks, eye movements or muscle artifacts were identified and removed. The EEG data were band-pass filtered (1–80 Hz, Butterworth, 3rd order),

downsampled to 1200 Hz, re-referenced to average reference, baseline corrected, and merged for the two conditions (Pre- and Post-rTMS). ICA (EEGLAB runica function) was applied to the combined dataset to remove additional residual artifacts [11]. The dataset was divided into the original Pre- and Post-rTMS conditions, and the epochs were re-segmented to the window of ±600 ms surrounding the TMS pulse. Lastly, signals from any disconnected or high-impedance channels were interpolated using spherical splines [36].

To assess the global cortical excitability, global-mean field power (GMFP) was calculated as the root-mean-squared value of the TEP across all electrodes in the 20–300 ms time interval after TMS stimulation [38]. This measure reflects the overall strength of TEPs across the entire cortex and provides insight into widespread cortical activity following stimulation [39]. To assess the local cortical excitability, the local mean field power (LMFP) was calculated across the electrodes close to the TMS coil in the 20–300 ms time interval after TMS stimulation [11], allowing for the assessment of the direct effects of TMS on specific cortical areas [39]. For M1 stimulation, C1, C3, Cp3, Cp1 electrodes were selected, likewise for DLPFC (AF3, F3, F1, FC3, FC1), ACC (FCz, Cz, FC1, FC2, C1, C2), and PSI (FC7, F C3, C7, C5, C3).

Time-frequency maps were extracted between 8 and 45 Hz using Morlet wavelets with 3.5 cycles, as implemented in the EEGLAB toolbox and previously reported [40]. The following TMS-evoked EEG parameters were extracted in the time-frequency domain:

- Event-related spectral perturbation (ERSP) was calculated to quantify power amplitudes in the frequency domain. ERSP was computed from the time-frequency maps as the average spectral power ratio of individual EEG trials relative to the pre-stimulus period (−600 to −50 ms). ERSP allows the identification of the changes in power as a function of time and frequency [8,40]. The significance of ERSP maps with respect to the baseline was assessed by bootstrapping samples from the pre-stimulus period (500 permutations, two-sided comparison, p-value <0.05 after false discovery rate (FDR) correction for multiple comparisons). Mean power spectra were then calculated by averaging significant ERSP values across electrodes and time samples (Fig. 2B and Supplementary Figs. 1B, 2B, 3B). ERSP quantified changes in evoked power across specific frequency bands as a function of time [41], to help identify how different oscillatory rhythms responded to TMS and providing insights into how rTMS influences brain rhythms.
- Inter-trial coherence (ITC) was extracted as a measure of phase synchronization. ITC was calculated by normalizing the complex-valued single-trial time-frequency values by their corresponding moduli and taking the absolute value of the across-trials averaged results. The significance of ITC maps concerning the baseline was assessed by bootstrapping samples from the pre-stimulus period (500 permutations, one-sided p-value <0.05 after FDR), and significant ITC values were averaged across electrodes, time samples, and frequency bands (Fig. 2C and Supplementary Figs. 1C, 2C, 3C). ITC measured the consistency of phase alignment across trials, with higher values (close to 1) indicating phase-locked neural responses to TMS [41] across trials and is a surrogate for functional connectivity in TMS-EEG studies.

The time-frequency analysis focused on three distinct frequency bands: α (8–13 Hz), low-β (14–24 Hz), and high-β (25–35 Hz). The division into these bands was based on an examination of the ERSP and ITC time-frequency plots, which identified distinct peaks of evoked activity centered around 20 Hz and 30 Hz (Fig. 2; Supplementary Figs. 1, 2, and 3). To better capture these oscillatory dynamics, the EEG beta frequency range was divided into low-β and high-β intervals, consistent with previous findings that underscore the need to discriminate between these intervals in TMS-EEG studies [42,43]. For each frequency band, ERSP and ITC values were then averaged over temporal intervals and spatial regions of interest, chosen according to the results of a non-parametric cluster-based statistical comparison between active and sham stimulation (see the *Statistical Analysis* section).

To investigate if the observed changes in ERSP and ITC were not due to volume conduction from a common source activity, the weighted Phase Lag Index (wPLI) was also calculated. wPLI assesses the asymmetry of the phase difference distribution between pairs of EEG signals, which is indicative of phase synchronization between electrodes free from zero-lag components. For each session, wPLI was calculated as described by Vinck et al. (2011) [44]. The resulting connectivity matrix was then averaged across each time window of interest for both electrodes belonging to the same spatial cluster (intra-cluster) and for different clusters (inter-cluster).

Statistical analysis

In order to identify temporal intervals and spatial clusters that exhibit significant differences between the sham and rTMS conditions, the spatiotemporal maps of ERSP and ITC averaged in each frequency band were subject-normalized by subtracting pre-rTMS maps from post-rTMS maps and compared between active and sham rTMS using a non-parametric permutation test, corrected for multiple comparisons through cluster-based statistics [45]. This analysis, as implemented in the open-source FieldTrip Toolbox [46], consisted of two main steps [45]: 1) First-level t-statistics were computed for each spatiotemporal data point (each combination of time and electrode), which established the threshold for identifying significant samples ($p < 0.05$, two-sided). Significant spatiotemporal samples were grouped into clusters based on spatial (minimum of two adjacent electrodes) and temporal proximity. 2) The sum of the first-level statistics within each cluster was calculated as the cluster-level statistic. To determine the significance of these clusters, a Monte Carlo permutation approach was used, where 5000 random permutations were generated by shuffling the data across conditions. The observed cluster-level statistic was compared to the distribution of the maximum cluster-level statistics from these permutations. Clusters were considered significant if their summed statistics exceeded the 95th percentile of the permuted values. Finally, for each frequency band, the ERSP and ITC values were averaged over the corresponding time intervals and spatial cluster identified by the cluster analysis.

The distributions of averaged ERSP and ITC values, as well as the measures of cortical excitability, MEP amplitudes, and mean wPLI, were subjected to the Shapiro-Wilk normality test. The null hypothesis that samples came from a normal distribution was rejected for several of the raw distributions ($p < 0.01$). However, the normality hypothesis was not rejected for the subject-normalized distributions of absolute changes, calculated as the difference between the post-rTMS and pre-rTMS values. Therefore, to satisfy the normality assumption required for parametric testing, and to focus on rTMS induced changes while reducing data variability, absolute changes with respect to pre-rTMS were used for all metrics in the final statistical comparisons between active and sham stimulations. The paired Student's t-test was employed for these comparisons. Matlab and Statistical Package for Social Sciences (SPSS, version 25; IBM) were used for all statistical analyses. Data are presented as mean ± standard deviation.

Results

All participants completed sham and active rTMS to M1 and TMS-EEG assessments without experiencing adverse effects. The TMS-evoked potential intensities for each cortical area and the average number of artifact-free epochs are detailed in Supplementary Tables 1 and 2 The rTMS intensities were 62.1 ± 8.3 % for sham and 62.5 ± 8.1 % for active rTMS. This slight increase in intensity for the rTMS was necessary due to differences in the coil types used, with the 70-mm Double Air Film Coil requiring a higher output to achieve the same stimulation efficacy as the D70^2 coil. The rMT was assessed with both coils to ensure consistency in the intensity relative to the rMT across procedures. Data from three

subjects were excluded due to TMS-EPs peak-to-peak amplitude not reaching 6 μV [7].

Effects of M1 rTMS on M1 TMS-EEG and MEPs

Local and global mean field power analyses did not show significant differences between active and sham rTMS (Supplementary Fig. 4). Data-driven analyses for group-level comparisons of ERSP and ITC revealed a difference in the high-β band in the ITC in the time interval 48–83 ms. Furthermore, in the low-β band, ERSP also revealed a difference in the time interval 86–144 ms. Topographic plots for M1 TMS revealed the electrodes where differences were present (Fig. 3), allowing their grouping into distinct clusters and two equal time intervals: early (48–83 ms) and late (86–144 ms) intervals. A significant increase in high-β band early (48–83 ms) phase reset (ITC) after active rTMS was detected compared to sham in the left central cluster ($t_{(16)} = 3.258$; $p = 0.005$; electrodes: C3, C5, Cp3, and Cp5), in the left frontal cluster ($t_{(16)} = 2.446$; $p = 0.026$; electrodes: Af3, F1 and F3), and in the right frontal cluster ($t_{(16)} = 4.052$; $p = 0.001$; electrodes: Af4, F2 and F4). These changes were temporally followed (86–144 ms) by an increase in lower-β band later power (ERSP) after active rTMS compared with sham in the left centro-parietal cluster ($t_{(16)} = 2.943$; $p = 0.009$; electrodes: C1, C3, Cp1, Cp3, P1, and P3), right centro-parietal cluster ($t_{(16)} = 3.683$; $p = 0.002$; electrodes: C2, C4, Cp2, Cp4, P2, and P4), and left prefrontal cluster ($t_{(16)} = 4.684$; $p = 0.001$; electrodes: Fp1, Af3, and Af7) (non-normalized parameters are reported in Tables 1 and 2).

Phase-based connectivity analyses confirmed the sequential events described above in high-β band wPLI after active rTMS compared with sham between the left central cluster (peri-stimulation site) and left prefrontal cluster both at early ($t_{(16)} = 2.490$; $p = 0.024$) and late ($t_{(16)} = 2.181$; $p = 0.044$) time intervals. These findings were similarly followed by an increase in high-β ($t_{(16)} = 3.533$; $p = 0.003$) and low-β ($t_{(16)} = 2.511$; $p = 0.023$) band wPLI after active rTMS between the left central cluster (peri-stimulation site) and right centro-parietal cluster at the late time interval (non-normalized parameters are reported in Table 3). Absolute changes in MEP amplitudes were not significant (Supplementary Table 3).

Effects of M1 rTMS on DLPFC, ACC, and PSI TMS-EEG

Local and global mean field power analysis (Supplementary Figs. 5, 6, and 7) and the time-frequency analyses did not show any significant difference between active and sham rTMS in any of the three other cortical areas proved with TMS-EEG.

Table 1
Mean ± standard deviation of the high-β band inter-trial coherence (0–1) for each condition before and immediately after repetitive transcranial magnetic stimulation (rTMS) to the primary motor cortex. Two regions in the 48–83 ms time interval were selected based on significant effects when analyzing the differences in non-parametric permutation tests.

Cluster	Condition	Pre-rTMS	Post-rTMS	Absolute change
Left central	Sham	0.46 ± 0.17	0.44 ± 0.20	−0.02 ± 0.08
	Active	0.44 ± 0.17	0.48 ± 0.16	0.04 ± 0.05
	p-value			0.005
Left frontal	Sham	0.43 ± 0.18	0.40 ± 0.18	−0.02 ± 0.09
	Active	0.41 ± 0.16	0.46 ± 0.16	0.04 ± 0.07
	p-value			0.026
Right frontal	Sham	0.38 ± 0.17	0.35 ± 0.15	−0.03 ± 0.09
	Active	0.35 ± 0.17	0.38 ± 0.16	0.04 ± 0.06
	p-value			0.001

Table 2
Mean ± standard deviation of the low-β band event-related spectral perturbation (dB) for each condition before and immediately after repetitive transcranial magnetic stimulation (rTMS) to the primary motor cortex. Four regions in the 86–144 ms time interval were selected based on significant effects when analyzing the differences in non-parametric permutation tests.

Cluster	Condition	Pre-rTMS	Post-rTMS	Absolute change
Left centro-parietal	Sham	1.76 ± 1.15	1.27 ± 1.06	−0.49 ± 0.69
	Active	1.74 ± 1.50	1.75 ± 1.19	0.01 ± 0.69
	p-value			0.009
Left prefrontal	Sham	1.17 ± 1.01	0.83 ± 0.81	−0.35 ± 0.50
	Active	1.07 ± 0.82	1.33 ± 0.66	0.26 ± 0.56
	p-value			0.001
Right centro-parietal	Sham	1.00 ± 0.84	0.73 ± 0.85	−0.28 ± 0.69
	Active	0.84 ± 0.71	1.23 ± 0.67	0.39 ± 0.66
	p-value			0.002

Discussion

The present study provides original insights into both the local and remote connectivity changes persisting after a session of high-frequency M1-rTMS. Initial increases in faster β-band intertrial coherence occurred in electrodes around M1 and in the ipsilateral frontal and homologous contralateral hemispheres. Initial increases in intertrial coherence were followed by increases in power in the slower β-band, observable locally in the prefrontal ipsilateral and peri-motor contralateral hemispheres. Phase-based connectivity analyses further supported that active rTMS increased phase lagging between the stimulated M1 area and remote

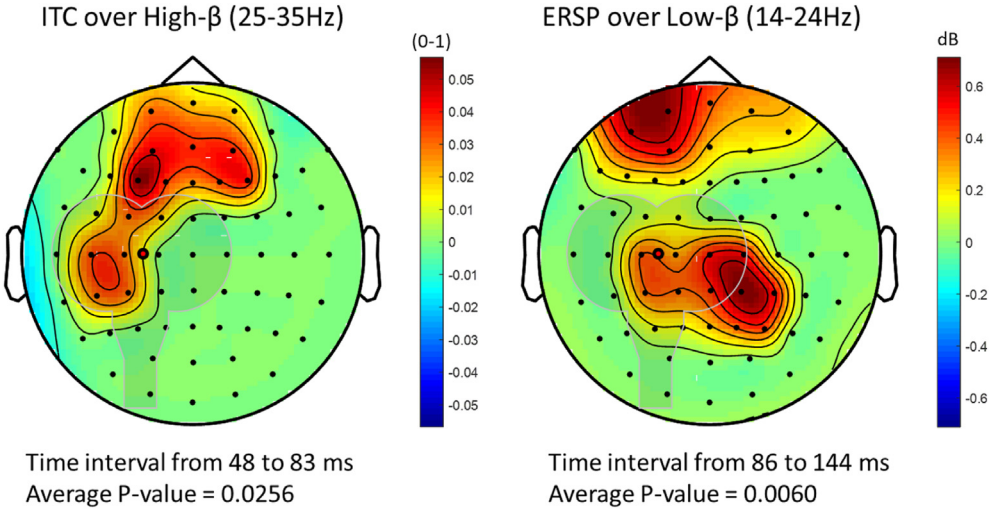

Fig. 3. Topographic maps of the average difference between active and sham rTMS for the spatiotemporal clusters of ITC (left, high-β band) and ERSP (right, low-β band) found significant. A positive change in these maps reflects an increase in oscillatory power or phase synchronization, indicating that the brain response to TMS has become more synchronized and stronger relative to baseline in a particular frequency band. Conversely, a negative change indicates a decrease in power or synchronization, suggesting reduced activity or phase alignment in the respective frequency band. Average P-values and time intervals of the significant clusters are displayed below.

Table 3
Mean ± standard deviation of the weighted phase lag index (0–1) for each condition before and immediately after repetitive transcranial magnetic stimulation (rTMS) to the primary motor cortex. Two regions were selected based on significant effects when analyzing the differences in event-related spectral perturbation and inter-trial coherence.

Clusters	Condition	Pre-rTMS	Post-rTMS	Absolute change
High-β band: left central-left prefrontal (time interval 48–83 ms)	Sham	0.35 ± 0.13	0.32 ± 0.10	−0.03 ± 0.08
	Active	0.32 ± 0.12	0.35 ± 0.13	0.03 ± 0.07
	p-value			0.024
High-β band: left central-left prefrontal (time interval 86–144 ms)	Sham	0.17 ± 0.05	0.14 ± 0.03	−0.03 ± 0.05
	Active	0.15 ± 0.06	0.17 ± 0.06	0.02 ± 0.07
	p-value			0.044
Low-β band: left central-right centro-parietal (time interval 86–144 ms)	Sham	0.21 ± 0.07	0.18 ± 0.05	−0.03 ± 0.07
	Active	0.18 ± 0.04	0.21 ± 0.05	0.02 ± 0.05
	p-value			0.023
High-β band: left central-right centro-parietal (time interval 86–144 ms)	Sham	0.15 ± 0.05	0.14 ± 0.03	−0.01 ± 0.04
	Active	0.14 ± 0.03	0.17 ± 0.04	0.03 ± 0.04
	p-value			0.003

extra-motor areas. Contrarily, cortical responses to extra-motor stimulations (DLPFC, ACC, and PSI) were not significantly affected by rTMS to M1, suggesting that connectivity changes were mainly measurable in M1-related networks.

Effects of M1 rTMS on M1 β-band oscillatory activity

The current results demonstrated that active 10 Hz rTMS to M1 did not significantly enhance the α-band oscillation in electrodes close to the stimulation area via causal entrainment of brain oscillations like previously reported for the parietal cortex [47] or under continuous and intermittent TBS [14–16]. Instead, M1-rTMS sequentially increased high β-band oscillatory synchronization and then low β-band oscillatory power. This is the first account for the TMS-EEG changes in cortical excitability and connectivity changes after M1 rTMS, and it builds upon pioneering studies investigating the effects of single-pulse TMS, paired-pulses, or short trains of TMS pulse. These previous studies reported a synchronized, rhythmic brain activity, often oscillating at the natural frequency of the targeted region [8,47]. Specifically, at the M1 region, single-pulse TMS has been shown to trigger a transient period of synchronized beta activity (15–30 Hz) not only at the stimulation site [48] but also at distant regions [49]. Additionally, an increase in beta power has been observed following a 15-min train of low-frequency (0.6 Hz) rTMS at 90 % of rTMS [50]. Single pulses TMS or short trains of rhythmic or arhythmic rTMS to M1 at ~18 Hz (peak of individual participant's resting-state beta oscillation) also triggered an increase in beta power on resting EEG, independently of the pattern of stimulation [51]. All these results, and our own, corroborate the concept that beta oscillatory response after M1-rTMS reflects potentiation of the endogenous M1′s β-band natural oscillatory activity, regardless of rTMS frequency or rhythmicity. This supports the idea that the after-effects of rTMS delivered at frequencies ~10–20 Hz are related to the M1 main frequency rather than to effects linked to the stimulation frequency band. Furthermore, the observed increase in β-band oscillatory in the M1 region persisting after the end of the stimulation session can be attributed to mechanisms underlying Hebbian synaptic plasticity. rTMS induces cortical plastic changes by repetitively depolarizing myelinated axons in M1 [2], likely reflected in the enhanced β-band oscillatory activity. This is linked to the function of β oscillations, which play a key role in coordinating motor planning and learning processes [52] and reaching the contralateral motor cortex likely via transcallosal projections [53]. Several studies suggest that high frequency rTMS can influence the excitability of contralateral homologous regions through interhemispheric facilitation mechanisms [54], leading to changes in the contralateral hemisphere's oscillatory dynamics. This could explain why increased β synchronization in M1 might also impact its contralateral homolog, facilitating motor coordination across hemispheres.

An important finding of the current study is the increase in high β-band oscillatory synchronization after active rTMS. ITC is a measure computed from single-trial cortical responses, reflecting the temporal and spectral synchronization within the EEG response and indicating the extent to which underlying phase-locking occurs, providing a direct measure of cortical synchrony [36]. High β-band oscillatory synchronization in cortical regions has previously been demonstrated to play a crucial role in interregional cortical communication and function, and their coordination across regions and inter-regional coordination jointly improve behavioural performance [55]. Thus, the increased high β-band oscillatory synchronization found here could be hypothesized as an increase in communication-through-coherence between M1 and its connected areas [56]. The communication-through-coherence theory suggests that brain rhythms encompass distinctly increased excitation and inhibition phases, and inputs are most effective when timed to coincide with excitation phases and not with phases of inhibition [57]. This optimal timing can occur if the inputs are rhythmic, thereby influencing synchronized rhythms in the target brain regions [55].

Another main finding of the current study was the increase in high-β synchronization after active rTMS, followed by an increase in low-β band power. This temporal interaction between cortical rhythms may indicate a cross-frequency coupling from a faster to a slower rhythmic state. It is well-known that cross-frequency coupling is a crucial mechanism for interaction between the many discrete frequencies of rhythm observable in neocortical networks [58]. In animal and human studies, phase-amplitude coupling has been observed, converging on the notion that it plays an important functional role in local computation and long-range communication in large-scale brain networks [59].

A final relevant finding of the current study was the increased β-band connectivity, as measured by wPLI, across several different clusters of electrodes after active rTMS. The phase-based connectivity analysis suggests that this effect was not produced by volume conduction and that the increase in β-band oscillatory synchronization and power after rTMS do not originate from the directly targeted cortex but also from remote cortical regions, allowing the inference of effective connectivity changes and driving the changes in its interconnected areas. This is supported by a large body of animal and human evidence [20,60] showing that pain analgesia and somatosensory effects of M1 stimulation are dependent on the engagement of extra-motor areas and diffuse effects such as the release of endogenous opioids [61]. It was suggested that M1 has areas that are highly connected to the extra motor (e.g., cognitive control, interoceptive, pain modulatory) network [62], which could be central to the clinical effects reported to date after M1 rTMS [63].

Effects of M1 rTMS on DLPFC, ACC, and PSI oscillatory activity

No significant changes in cortical excitability or oscillations were found when TMS stimulated DLPFC, ACC, and PSI targets after M1 rTMS at 10 Hz. Previous concurrent TMS-fMRI studies have shown that TMS can induce neurovascular responses in functionally connected non-motor areas, including the insula, cingulate cortex, and frontal cortices [17,64]. For instance, a recent study has shown that TMS over M1, synchronized with fMRI acquisition, led to increased activation in the bilateral insula [18]. Additionally, dynamic causal modeling indicated direct inputs from M1 to the ACC [65]. Despite this evidence of activation in connected cortical regions, our study did not capture any neuroplastic effects in these areas following high-frequency rTMS to M1. This may be because M1, the directly stimulated region, is more responsive to rTMS. In

contrast, functionally connected regions like the DLPFC, ACC, and PSI might require multiple rTMS sessions to induce noticeable neuroplastic changes. Alternatively, the effects in these regions could be more transient, being exclusively present and measurable during the stimulation session, as they are likely influenced indirectly by M1 stimulation. Future studies should consider targeting a single cortical region before and after a single session of rTMS for more accurate assessments.

Finally, the variability observed in the temporal (time intervals) and spatial (electrode localization) aspects of the results may reflect distinct neural responses across different targets. This variability indicates that the TMS responses capture target-specific neural dynamics rather than being dominated by non-neural artifacts like TMS-related or auditory and somatosensory evoked potentials [8,35,66,67]. If artifacts were the main component, more uniform, less variable patterns across different targets and frequencies were expected.

Limitations

The main limitation of the present study is the absence of behavioral assessment. This was an active choice in the design of the study, given that the connectivity changes after M1 rTMS were mainly unknown, while the behavioral effects after M1 stimulation have been previously described [68].

Furthermore, only M1 was targeted with rTMS. Considering that responsiveness to active rTMS may vary significantly across different cortical areas based on endogenous oscillation, future research should investigate the effects of targeting different cortical areas, such as DLPFC, ACC, or PSI, which could induce different cortical responses.

Given the violation of the normality assumption and the large variance in cortical oscillation and connectivity between subjects and days—variability that is expected due to the dynamic nature of the brain [69]—repeated measures ANOVA was not applied, as it may not have been the most appropriate method for analyzing changes in brain responses between real and sham rTMS sessions. Cortical oscillations and connectivity can fluctuate significantly across individuals and from day to day [69], so focusing on post-pre differences – for which the normality assumption was not violated – provided a more reliable and robust approach. This allowed us to account for the inherent variability and effectively address the core research question: whether rTMS induces measurable changes in brain connectivity.

Finally, only 10 participants underwent TMS-EEG targeting the ACC and PSI since the post-rTMS effect on M1 is short-lasting [70]. Future studies should include larger sample sizes, lower number of cortical targets in the same experimental session and extend the duration of rTMS sessions to better capture the potential long-term effects on connectivity and cortical excitability in M1 and extra-motor areas. Additionally, multiple-day study designs could explore how repeated sessions of rTMS influence cortical networks over time, providing more robust evidence for the sustained effects of rTMS on brain plasticity.

Compared to sham-rTMS, active M1 rTMS engaged an enhanced TMS-synchronization, followed by an increase in TMS-evoked power amplitude occurring within M1 main frequencies and spreading to remote connected areas.

Data availability

All the data will be available upon reasonable request from the corresponding author.

Author contributions

Enrico De Martino: Conceptualization, Methodology, Formal analysis, Investigation, Data curation, Visualization, Writing- Original draft preparation; Writing - Review & Editing; Project administration; **Adenauer Girardi Casali**: Methodology, Software; Formal analysis; Data Curation; Visualization, Writing - Review & Editing; **Bruno Andry Nascimento Couto**: Software, Formal analysis, Data Curation, Visualization, Writing - Review & Editing, Visualization; **Thomas Graven-Nielsen**: Conceptualization, Methodology, Writing - Review & Editing, Funding acquisition; **Daniel Ciampi de Andrade**: Conceptualization, Methodology, Visualization, Writing - Original draft preparation; Writing - Review & Editing; Project administration, Funding acquisition.

Funding

The Center for Neuroplasticity and Pain (CNAP) is supported by the Danish National Research Foundation (DNRF121). The current study is supported by a Novo Nordisk (Grant NNF21OC0072828) and ERC Horizon Europe Consolidator grant (PersoNINpain 101087925).

Declaration of competing interests

The authors declare no conflict of interest related to the publication.

Appendix A. Supplementary data

Supplementary data to this article can be found online at https://doi.org/10.1016/j.neurot.2024.e00497.

References

[1] Lefaucheur JP, Aleman A, Baeken C, Benninger DH, Brunelin J, Di Lazzaro V, et al. Evidence-based guidelines on the therapeutic use of repetitive transcranial magnetic stimulation (rTMS): an update (2014–2018). Clin Neurophysiol 2020;131:474–528. https://doi.org/10.1016/j.clinph.2019.11.002.

[2] Siebner HR, Funke K, Aberra AS, Antal A, Bestmann S, Chen R, et al. Transcranial magnetic stimulation of the brain: what is stimulated? – a consensus and critical position paper. Clin Neurophysiol 2022;140:59–97. https://doi.org/10.1016/j.clinph.2022.04.022.

[3] Klomjai W, Katz R, Lackmy-Vallée A. Basic principles of transcranial magnetic stimulation (TMS) and repetitive TMS (rTMS). Ann Phys Rehabil Med 2015;58:208–13. https://doi.org/10.1016/j.rehab.2015.05.005.

[4] Mhalla A, Baudic S, Ciampi de Andrade D, Gautron M, Perrot S, Teixeira MJ, et al. Long-term maintenance of the analgesic effects of transcranial magnetic stimulation in fibromyalgia. Pain 2011;152:1478–85. https://doi.org/10.1016/j.pain.2011.01.034.

[5] Maeda F, Keenan JP, Tormos JM, Topka H, Pascual-Leone A. Interindividual variability of the modulatory effects of repetitive transcranial magnetic stimulation on cortical excitability. Exp Brain Res 2000;133:425–30. https://doi.org/10.1007/s002210000432.

[6] Magnuson J, Ozdemir MA, Mathieson E, Kirkman S, Passera B, Rampersad S, et al. Neuromodulatory effects and reproducibility of the most widely used repetitive transcranial magnetic stimulation protocols. PLoS One 2023;18(6):e0286465. https://doi.org/10.1371/journal.pone.0286465.

[7] Casarotto S, Fecchio M, Rosanova M, Varone G, D'Ambrosio S, Sarasso S, et al. The rt-TEP tool: real-time visualization of TMS-Evoked Potentials to maximize cortical activation and minimize artifacts. J Neurosci Methods 2022;370:109486. https://doi.org/10.1016/j.jneumeth.2022.109486.

[8] Rosanova M, Casali A, Bellina V, Resta F, Mariotti M, Massimini M. Natural frequencies of human corticothalamic circuits. J Neurosci 2009;29:7679–85. https://doi.org/10.1523/JNEUROSCI.0445-09.2009.

[9] Tremblay S, Rogasch NC, Premoli I, Blumberger DM, Casarotto S, Chen R, et al. Clinical utility and prospective of TMS – EEG. Clin Neurophysiol 2019;130:802–44. https://doi.org/10.1016/j.clinph.2019.01.001.

[10] Pfurtscheller G, Stancfik Jr A, Edlinger G. On the existence of different types of central beta rhythms below 30 Hz. Electroencephalogr Clin Neurophysiol 1997 Apr;102(4):316–25. https://doi.org/10.1016/s0013-4694(96)96612-2.

[11] Fecchio M, Pigorini A, Comanducci A, Sarasso S, Casarotto S, Premoli I, et al. The spectral features of EEG responses to transcranial magnetic stimulation of the primary motor cortex depend on the amplitude of the motor evoked potentials. PLoS One 2017;12:1–15. https://doi.org/10.1371/journal.pone.0184910.

[12] Torrecillos F, Falato E, Pogosyan A, West T, Di Lazzaro V, Brown P. Motor cortex inputs at the optimum phase of beta cortical oscillations undergo more rapid and less variable corticospinal propagation. J Neurosci 2020;40:369–81. https://doi.org/10.1523/JNEUROSCI.1953-19.2019.

[13] Forschack N, Nierhaus T, Müller MM, Villringer A. Alpha-band brain oscillations shape the processing of perceptible as well as imperceptible somatosensory stimuli during selective attention. J Neurosci 2017;37:6983–94. https://doi.org/10.1523/JNEUROSCI.2582-16.2017.

[14] Vernet M, Bashir S, Yoo WK, Perez JM, Najib U, Pascual-Leone A. Insights on the neural basis of motor plasticity induced by theta burst stimulation from TMS-EEG. Eur J Neurosci 2013;37:598–606. https://doi.org/10.1111/ejn.12069.

[15] Rocchi L, Ibáñez J, Benussi A, Hannah R, Rawji V, Casula E, et al. Variability and predictors of response to continuous theta burst stimulation: a TMS-EEG study. Front Neurosci 2018;12. https://doi.org/10.3389/fnins.2018.00400.
[16] Bai Z, Zhang J, Fong KNK. Intermittent theta burst stimulation to the primary motor cortex reduces cortical inhibition: a TMS-EEG study. Brain Sci 2021;11. https://doi.org/10.3390/brainsci11091114.
[17] Bergmann TO, Varatheeswaran R, Hanlon CA, Madsen KH, Thielscher A, Siebner HR. Concurrent TMS-fMRI for causal network perturbation and proof of target engagement. Neuroimage 2021;237. https://doi.org/10.1016/j.neuroimage.2021.118093.
[18] Jung JY, Bungert A, Bowtell R, Jackson SR. Modulating brain networks with transcranial magnetic stimulation over the primary motor cortex: a concurrent TMS/fMRI study. Front Hum Neurosci 2020;14. https://doi.org/10.3389/fnhum.2020.00031.
[19] Gordon EM, Chauvin RJ, Van AN, Rajesh A, Nielsen A, Newbold DJ, et al. A somato-cognitive action network alternates with effector regions in motor cortex. Nature 2023;617(7960):351–9. https://doi.org/10.1038/s41586-023-05964-2.
[20] Pagano RL, Fonoff ET, Dale CS, Ballester G, Teixeira MJ, Britto LRG. Motor cortex stimulation inhibits thalamic sensory neurons and enhances activity of PAG neurons: possible pathways for antinociception. Pain 2012;153:2359–69. https://doi.org/10.1016/j.pain.2012.08.002.
[21] Butti C, Hof PR. The insular cortex: a comparative perspective. Brain Struct Funct 2010;214:477–93. https://doi.org/10.1007/s00429-010-0264-y.
[22] Deen B, Pitskel NB, Pelphrey KA. Three systems of insular functional connectivity identified with cluster analysis. Cerebr Cortex 2011;21:1498–506. https://doi.org/10.1093/cercor/bhq186.
[23] Chowdhury NS, Millard SK, De Martino E, Boye Larsen D, Schabrun SM, Ciampi de Andrade D, et al. Posterior-superior insula repetitive transcranial magnetic stimulation reduces experimental tonic pain and pain-related cortical inhibition in humans. bioRvix 2024. https://doi.org/10.1101/2024.05.14.594260.
[24] Morecraft RJ, Van Hoesen GW. Convergence of limbic input to the cingulate motor cortex in the rhesus monkey. Brain Res Bull 1998;45(2):209–32. https://doi.org/10.1016/s0361-9230(97)00344-4.
[25] Cieslik EC, Zilles K, Caspers S, Roski C, Kellermann TS, Jakobs O, et al. Is there one DLPFC in cognitive action control? Evidence for heterogeneity from Co-activation-based parcellation. Cerebr Cortex 2013;23:2677–89. https://doi.org/10.1093/cercor/bhs256.
[26] Wang Y, Cao N, Lin Y, Chen R, Zhang J. Hemispheric differences in functional interactions between the dorsal lateral prefrontal cortex and ipsilateral motor cortex. Front Hum Neurosci 2020;14. https://doi.org/10.3389/fnhum.2020.00202.
[27] Hasan A, Galea JM, Casula EP, Falkai P, Bestmann S, Rothwell JC. Muscle and timing-specific functional connectivity between the dorsolateral prefrontal cortex and the primary motor cortex. J Cogn Neurosci 2013;25:558–70. https://doi.org/10.1162/jocn_a_00338.
[28] Rossi S, Antal A, Bestmann S, Bikson M, Brewer C, Brockmöller J, et al. Safety and recommendations for TMS use in healthy subjects and patient populations, with updates on training, ethical and regulatory issues: expert Guidelines. Clin Neurophysiol 2021;132:269–306. https://doi.org/10.1016/j.clinph.2020.10.003.
[29] Jung SH, Shin JE, Jeong YS, Shin HI. Changes in motor cortical excitability induced by high-frequency repetitive transcranial magnetic stimulation of different stimulation durations. Clin Neurophysiol 2008;119:71–9. https://doi.org/10.1016/j.clinph.2007.09.124.
[30] Rossini PM, Burke D, Chen R, Cohen LG, Daskalakis Z, Iorio R Di, et al. Non-invasive electrical and magnetic stimulation of the brain, spinal cord, roots and peripheral nerves: basic principles and procedures for routine clinical and research application. An updated report from an I.F.C.N. Committee. Clin Neurophysiol 2015;126:1071–107. https://doi.org/10.1016/j.clinph.2015.02.001.
[31] Russo S, Sarasso S, Puglisi GE, Dal Palù D, Pigorini A, Casarotto S, et al. Taac - TMS Adaptable Auditory Control: a universal tool to mask TMS clicks. J Neurosci Methods 2022;370:109491. https://doi.org/10.1016/j.jneumeth.2022.109491.
[32] Mylius V, Ayache SS, Ahdab R, Farhat WH, Zouari HG, Belke M, et al. Definition of DLPFC and M1 according to anatomical landmarks for navigated brain stimulation: inter-rater reliability, accuracy, and influence of gender and age. Neuroimage 2013;78:224–32. https://doi.org/10.1016/j.neuroimage.2013.03.061.
[33] Carmi L, Alyagon U, Barnea-Ygael N, Zohar J, Dar R, Zangen A. Clinical and electrophysiological outcomes of deep TMS over the medial prefrontal and anterior cingulate cortices in OCD patients. Brain Stimul 2018;11:158–65. https://doi.org/10.1016/j.brs.2017.09.004.
[34] da Cunha PHM, Tanaka H, Lapa JD da S, Dongyang L, Boa Sorte AA, Pereira TMR, et al. The fast-posterior superior insula (Fast-PSI): a neuronavigation-free targeting method for non-invasive neuromodulation. Brain Stimul 2022;15:1178–80. https://doi.org/10.1016/j.brs.2022.08.009.
[35] Casarotto S, Lauro LJR, Bellina V, Casali AG, Rosanova M, Pigorini A, et al. EEG responses to TMS are sensitive to changes in the perturbation parameters and repeatable over time. PLoS One 2010;5. https://doi.org/10.1371/journal.pone.0010281.
[36] Delorme A, Makeig S. Eeglab : an open source toolbox for analysis of single-trial EEG dynamics including independent component analysis. J Neurosci Methods 2004;134:9–21. https://doi.org/10.1016/j.jneumeth.2003.10.009.
[37] D'Ambrosio S, Jiménez-Jiménez D, Silvennoinen K, Zagaglia S, Perulli M, Poole J, et al. Physiological symmetry of transcranial magnetic stimulation-evoked EEG spectral features. Hum Brain Mapp 2022;43:5465–77. https://doi.org/10.1002/hbm.26022.
[38] Lehmann D, Skrandies W. Reference-free identification of components of checkerboard-evoked multichannel potential fields. Electroencephalogr Clin Neurophysiol 1980;48:609–21. https://doi.org/10.1016/0013-4694(80)90419-8.
[39] Komssi S, Kähkönen S, Ilmoniemi RJ. The effect of stimulus intensity on brain responses evoked by transcranial magnetic stimulation. Hum Brain Mapp 2004;21:154–64. https://doi.org/10.1002/hbm.10159.
[40] Donati FL, Mayeli A, Sharma K, Janssen SA, Lagoy AD, Casali AG, et al. Natural oscillatory frequency slowing in the premotor cortex of early-course schizophrenia patients: a TMS-EEG study. Brain Sci 2023;13. https://doi.org/10.3390/brainsci13040534.
[41] Makeig S, Debener S, Onton J, Delorme A. Mining event-related brain dynamics. Trends Cognit Sci 2004;8:204–10. https://doi.org/10.1016/j.tics.2004.03.008.
[42] Donati FL, Kaskie R, Reis CC, D'Agostino A, Casali AG, Ferrarelli F. Reduced TMS-evoked fast oscillations in the motor cortex predict the severity of positive symptoms in first-episode psychosis. Prog Neuro-Psychopharmacol Biol Psychiatry 2021;111. https://doi.org/10.1016/j.pnpbp.2021.110387.
[43] Ferrarelli F, Kaskie RE, Graziano B, Reis CC, Casali AG. Abnormalities in the evoked frontal oscillatory activity of first-episode psychosis: a TMS/EEG study. Schizophr Res 2019;206:436–9. https://doi.org/10.1016/j.schres.2018.11.008.
[44] Vinck M, Oostenveld R, Van Wingerden M, Battaglia F, Pennartz CMA. An improved index of phase-synchronization for electrophysiological data in the presence of volume-conduction, noise and sample-size bias. Neuroimage 2011;55:1548–65. https://doi.org/10.1016/j.neuroimage.2011.01.055.
[45] Maris E, Oostenveld R. Nonparametric statistical testing of EEG- and MEG-data. J Neurosci Methods 2007;164:177–90. https://doi.org/10.1016/j.jneumeth.2007.03.024.
[46] Oostenveld R, Fries P, Maris E, Schoffelen JM. FieldTrip: open source software for advanced analysis of MEG, EEG, and invasive electrophysiological data. Comput Intell Neurosci 2011;2011. https://doi.org/10.1155/2011/156869.
[47] Thut G, Veniero D, Romei V, Miniussi C, Schyns P, Gross J. Rhythmic TMS causes local entrainment of natural oscillatory signatures. Curr Biol 2011;21:1176–85. https://doi.org/10.1016/j.cub.2011.05.049.
[48] Paus T, Sipila PK, Strafella AP. Synchronization of neuronal activity in the human primary motor cortex by transcranial magnetic stimulation: an EEG study. J Neurophysiol 2001;86:1983–90. https://doi.org/10.1152/jn.2001.86.4.1983.
[49] Fuggetta G, Fiaschi A, Manganotti P. Modulation of cortical oscillatory activities induced by varying single-pulse transcranial magnetic stimulation intensity over the left primary motor area: a combined EEG and TMS study. Neuroimage 2005;27:896–908. https://doi.org/10.1016/j.neuroimage.2005.05.013.
[50] Van Der Werf YD, Paus T. The neural response to transcranial magnetic stimulation of the human motor cortex. I. Intracortical and cortico-cortical contributions. Exp Brain Res 2006;175:231–45. https://doi.org/10.1007/s00221-006-0551-2.
[51] Hannah R, Muralidharan V, Aron AR. Motor cortex oscillates at its intrinsic post-movement beta rhythm following real (but not sham) single pulse, rhythmic and arrhythmic transcranial magnetic stimulation. Neuroimage 2022;251. https://doi.org/10.1016/j.neuroimage.2022.118975.
[52] Barone J, Rossiter HE. Understanding the role of sensorimotor beta oscillations. Front Syst Neurosci 2021;15. https://doi.org/10.3389/fnsys.2021.655886.
[53] Daskalakis ZJ, Christensen BK, Fitzgerald PB, Roshan L, Chen R. The mechanisms of interhemispheric inhibition in the human motor cortex. J Physiol 2002;543:317–26. https://doi.org/10.1113/jphysiol.2002.017673.
[54] Tian D, Izumi SI. Interhemispheric facilitatory effect of high-frequency rTMS: perspective from intracortical facilitation and inhibition. Brain Sci 2022;12. https://doi.org/10.3390/brainsci12080970.
[55] Parto-Dezfouli M, Vezoli J, Bosman CA, Fries P. Enhanced behavioral performance through interareal gamma and beta synchronization. Cell Rep 2023;42. https://doi.org/10.1016/j.celrep.2023.113249.
[56] Fries P. A mechanism for cognitive dynamics: neuronal communication through neuronal coherence. Trends Cognit Sci 2005;9:474–80. https://doi.org/10.1016/j.tics.2005.08.011.
[57] Fries P. Rhythms for cognition: communication through coherence. Neuron 2015;88:220–35. https://doi.org/10.1016/j.neuron.2015.09.034.
[58] Roopun AK, Kramer MA, Carracedo LM, Kaiser M, Davies CH, Traub RD, et al. Temporal interactions between cortical rhythms. Front Neurosci 2008;2:145–54. https://doi.org/10.3389/neuro.01.034.2008.
[59] Canolty RT, Knight RT. The functional role of cross-frequency coupling. Trends Cognit Sci 2010;14:506–15. https://doi.org/10.1016/j.tics.2010.09.001.
[60] Kadono Y, Koguchi K, Okada K ichi, Hosomi K, Hiraishi M, Ueguchi T, et al. Repetitive transcranial magnetic stimulation restores altered functional connectivity of central poststroke pain model monkeys. Sci Rep 2021;11. https://doi.org/10.1038/s41598-021-85409-w.
[61] Maarrawi J, Peyron R, Mertens P, Costes N, Magnin M, Sindou M, et al. Motor cortex stimulation for pain control induces changes in the endogenous opioid system. Neurology 2007;69:827–34. https://doi.org/10.1212/01.wnl.0000269783.86997.37.
[62] Ciampi De Andrade D, Mhalla A, Adam F, Texeira MJ, Bouhassira D. Neuropharmacological basis of rTMS-induced analgesia: the role of endogenous opioids. Pain 2011;152:320–6. https://doi.org/10.1016/j.pain.2010.10.032.
[63] Attal N, Poindessous-Jazat F, De Chauvigny E, Quesada C, Mhalla A, Ayache SS, et al. Repetitive transcranial magnetic stimulation for neuropathic pain: a randomized multicentre sham-controlled trial. Brain 2021:3328–39. https://doi.org/10.1093/brain/awab208.
[64] Bestmann S, Baudewig J, Siebner HR, Rothwell JC, Frahm J. Subthreshold high-frequency TMS of human primary motor cortex modulates interconnected frontal motor areas as detected by interleaved fMRI-TMS. Neuroimage 2003;20:1685–96. https://doi.org/10.1016/j.neuroimage.2003.07.028.
[65] Hodkinson DJ, Bungert A, Bowtell R, Jackson SR, Jung JY. Operculo-insular and anterior cingulate plasticity induced by transcranial magnetic stimulation in the human motor cortex: a dynamic casual modeling study. J Neurophysiol 2021;125:1180–90. https://doi.org/10.1152/jn.00670.2020.

[66] Belardinelli P, Biabani M, Blumberger DM, Bortoletto M, Casarotto S, David O, et al. Reproducibility in TMS–EEG studies: a call for data sharing, standard procedures and effective experimental control. Brain Stimul 2019;12:787–90. https://doi.org/10.1016/j.brs.2019.01.010.

[67] Rocchi L, Di A, Brown K, Ib J, Casula E, Rawji V, et al. Brain Stimulation Disentangling EEG responses to TMS due to cortical and peripheral activations. Brain Stimul 2021;14:4–18. https://doi.org/10.1016/j.brs.2020.10.011.

[68] Kim YH, You SH, Ko MH, Park JW, Lee KH, Jang SH, et al. Repetitive transcranial magnetic stimulation-induced corticomotor excitability and associated motor skill acquisition in chronic stroke. Stroke 2006;37:1471–6. https://doi.org/10.1161/01.STR.0000221233.55497.51.

[69] Zrenner C, Desideri D, Belardinelli P, Ziemann U. Real-time EEG-defined excitability states determine efficacy of TMS-induced plasticity in human motor cortex. Brain Stimul 2018;11:374–89. https://doi.org/10.1016/j.brs.2017.11.016.

[70] Di Lazzaro V, Dileone M, Pilato F, Capone F, Musumeci G, Ranieri F, et al. Modulation of motor cortex neuronal networks by rTMS: comparison of local and remote effects of six different protocols of stimulation. J Neurophysiol 2011;105:2150–6. https://doi.org/10.1152/jn.00781.2010.